

TURBULENT TRANSPORT CHARACTERISTICS IN A LOW-SPEED BOUNDARY LAYER SUBJECTED TO ADVERSE PRESSURE

Alberto Ayala

Department of Mechanical and Aerospace Engineering
West Virginia University
P.O. Box 6106
Morgantown, WV 26506-6106

Bruce R. White and Dae-Seong Kim

Department of Mechanical and Aeronautical Engineering
University of California
One Shields Avenue
Davis, CA 95616-5294

Nader Bagheri

Department of Mechanical Engineering
California Maritime Academy, The California State University
P.O. Box 1392
Vallejo, CA 94590-0644

ABSTRACT

Thermal anemometry measurements were performed to evaluate the heat and momentum transport characteristics of wall turbulence over a slightly heated, smooth flat plate with a step-change in wall temperature. Single-wire, X-probe and triple-wire sensors were employed to measure mean and fluctuating velocity and temperature as well as Reynolds stress and heat flux productions. "Equilibrium" boundary layers were considered for mild ($\beta \approx 0.8$, $Re_\theta \approx 3500$) and moderate ($\beta \approx 1.8$, $Re_\theta \approx 3800$) adverse-pressure-gradient (APG) conditions for a wall-to-free-stream temperature difference ΔT of approximately 12°C. The base case for zero-pressure-gradient (ZPG) conditions ($\beta \approx 0$, $Re_\theta \approx 2700$) was also investigated. The origins of the momentum and thermal boundary layers did not coincide, resulting in a layer development $\Delta/\Delta T$ of approximately 0.8, 1.2 and 1.5 for ZPG, mild and moderate APG, respectively. Findings suggest that the mean flow field and the fluctuating streamwise and normal flow fields responded proportionally to the magnitude of the adverse-pressure gradient present. The failure of the law-of-the-wall for velocity for the APG conditions considered was not severe. And the equilibrium condition of the flow was maintained through a balance of adverse pressure and turbulent stress production. The Reynolds analogy was confirmed for ZPG conditions while, in adverse pressure, the turbulent stress production scaled with the streamwise heat flux. The heat flux production was found to be self-similar for the pressure gradient cases investigated.

INTRODUCTION

The subject of adverse-pressure-gradient flows is of interest since they occur often in practice. Appropriately, Nagano et al. (1991) remarked that "since adverse-pressure-gradient flows often occur in various kinds of fluid machinery, it is of both fundamental and practical

importance to investigate the adverse-pressure-gradient effects on the characteristics of turbulent boundary layers.” In addition, Spalart and Watmuff (1993) noted that “adverse gradients are of more practical interest – because of separation, of more theoretical interest – because the wall shear stress does not dominate the situation, and more delicate experimentally – because of their higher sensitivity to upstream conditions.” There have been a number of investigations focused on APG flows in addition to those conducted previously by our group (for example Ayala et al., 1997 and Lin, 1995). Turbulence contains a collection of large-scale coherent structures that have dimensions comparable to the boundary layer thickness. The term coherent structure refers to large-scale events that show significant correlation over a spatial region in the boundary layer. Watmuff (1989) and Lian (1990) observed that coherent structures in APG flow appeared to be larger and moved more violently than their zero-pressure-gradient (ZPG) counterparts. Nagano et al. (1998), (1991) and Nagano and Tagawa (1988) presented a comprehensive discussion on the effect of adverse pressure on the mean and fluctuating characteristics of the turbulent boundary layer. Blackwell et al. (1972) and Orlando et al. (1974) investigated the turbulent boundary layer in APG conditions and focused on the thermal and dynamic characteristics of the flow for various adverse pressure conditions. Our contribution, within the context of previous efforts, is intended to add to the existing experimental database on the subject. We do this by presenting direct and simultaneous measurements of thermal and dynamic events conducted with customized single triple-sensor probes. In this paper, we intend to present findings from our continued investigation of “equilibrium” adverse-pressure-gradient turbulent boundary layer flow. We will focus our attention specifically on the response of the mean and fluctuating flow to the presence of moderate adverse pressure. The reader is referred to Table 1 for a listing of the relevant test parameters.

EXPERIMENTAL METHODS

Experimental Facility

The open-return low-speed wind tunnel at the University of California at Davis shown in Figure 1 was used for this investigation. A complete description may be found in Ayala et al. (1997). Briefly, it has a 7.5 m overall length and a 17:1 contraction ratio of the bell-mouth nozzle section. The diffuser is 2.3 m long with a continuous transition from the rectangular test section to the circular fan housing. The test section (TS) is 3 m long by 0.3 m wide. The TS aspect ratio (TS-width/ δ) is 10 or more for the APG flows measured. The motor is capable of free-stream velocities ranging from 2.5 m/s to 25 m/s and a resulting TS free-stream turbulence intensity of about 1 % for ZPG conditions. A free-stream turbulence intensity of approximately 1.5 % was achieved for the two APG cases.

Heated-wall Design

The wind-tunnel floor consists of an unheated starting length and a section for tripping the flow. This makes the origins of the thermal and momentum boundary layers different. Individually heated aluminum plates span longitudinally along the tunnel floor. Insulating material, placed between plates, minimizes axial-heat conduction. Heating is achieved by means of heating elements placed directly underneath the aluminum plates. Conduction and radiation losses from the aluminum plates are estimated at approximately 3% of the heat input (Bagheri et al. 1995). The wind tunnel floor temperature distribution was monitored with type E miniature thermocouples calibrated in a Rosemount Constant-temperature Bath against a Platinum

Resistance Thermometer. The temperature distribution was monitored at three spanwise locations to ensure uniformity.

Instrumentation

TSI hot- and cold-wire probes controlled by standard TSI 1050 series CT and CC anemometers were used in this study. Single-wire measurements of streamwise velocity were made with a 1261A-T1.5 miniature boundary-layer probe with an upper frequency response of 600 kHz. The active sensor dimensions were 4 μm in diameter and 1.25 mm in length. Single-wire temperature measurements were obtained with a 1276-P0.5 subminiature straight probe with a 1.3 μm diameter and a 1 mm length. The typical upper frequency response for such a probe was 500 kHz. Reynolds stress measurements were conducted with a standard 1241-D344 tungsten X-probe with a 4 μm diameter and a 1.2 mm length. The triple-wire probes (1296BH-T1.5) consisted of a tungsten velocity X-probe (T1.5) and a platinum wire (P1) for temperature. The X-probe had a length of 1.2 mm and 4 μm diameter while the cold wire was 2.5 μm in diameter with a 1.2 mm length. The temperature wire was placed directly upstream of the X-probe at an axial separation distance of approximately 1 mm. The operation of the X-probe in a non-isothermal field was compensated to correct for temperature contamination. And the flow wake from the temperature wire did not have a measurable effect on the X-probe. Conversely, it was determined experimentally that the cold-wire temperature sensor performance was not affected by its proximity to the “heated” X-probe.

RESULTS AND DISCUSSION

Equilibrium Adverse-Pressure-Gradient Conditions

As originally stated by Clauser (1954), “equilibrium” APG boundary layers result in a one-parameter (β) family of “defect” profiles in the outer flow region, Spalart and Watmuff (1993). For these profiles, the corresponding development of the freestream flow is of the form $U_\infty = Cx^m$. In the present investigation, mild and moderate APG conditions were established and compared to equilibrium profiles available in the literature. Results for moderate APG conditions are shown in Figure 2 where Station 5 refers to the streamwise location where all measurements were conducted at a corresponding Re_x value of approximately 2×10^6 . This figure suggests good agreement of the present testing conditions relative to Clauser’s, (1954) original work. Similar agreement was found for the mild APG test case. The streamwise and spanwise flow development was checked and two-dimensionality confirmed via profile measurements at various locations.

Wall Temperature

The streamwise distribution of the non-uniform heat flux/constant-temperature condition along the flat-plate test section is illustrated in Figure 3. Wall heat flux measurements were made possible by calibrating the power input to individual heating elements in terms of the root mean square voltage drop across them and by subtracting the estimated heat losses. Results showed a St distribution consistent with that expected for a step change in constant surface temperature. The uniformity and two-dimensionality of the wall temperature distribution for the

current tests was checked and confirmed by monitoring the distribution at various spanwise locations in a similar procedure to that by Bagheri et al. (1995).

Velocity Measurements

Mean Flow Field. Figure 4 illustrates that the response of the mean flow to an increase in adverse pressure is confined to the outer flow region of the boundary layer, as expected. In the wall proximity, the uniqueness of the state of the mean flow for constant streamwise pressure is described by the law-of-the-wall where the scaling velocity u^* is typically determined from Clauser's technique. This technique is attractive because it relies on outer-flow profile measurements. However, Nagano et al. (1991) and Sparlart and Watmuff (1993) have contributed to the body of evidence that points to the failure of the law-of-the-wall for APG flows. Their findings suggest that, in strong adverse pressure ($\beta > 3$), the normalized mean velocity profile falls below the universal law-of-the-wall line. Thus, suggesting a potential underestimation of the wall shear stress u^* by Clauser's approach. This discrepancy was determined from data collected in the viscous sub-layer region in the range of $y^+ < 6$, which is not easily accessible in experiments. Fortunately, for the finite case of moderate adverse pressure in the range considered in the present study ($\beta=1.8$), the universality of the law-of-the-wall seems to be preserved even for APG flows and a u^* based on Clauser's technique.

Fluctuating Flow Field. Streamwise velocity fluctuations are presented in Figure 5 in the form of turbulence intensity (T.I.), U_{rms}/U_∞ , versus dimensional wall-normal distance, y , for ZPG, mild, and moderate APG conditions. The figure reflects a free-stream turbulence level of 1 to 1.5% and a rapid increase of the fluctuations towards the wall. As expected, it is evident that the presence of adverse pressure causes an increase in fluctuations in the core region of the boundary layer. In contrast, APG effects are damped out by the solid surface as indicated by the similarity of the three profiles near the wall. When these fluctuations are normalized by the wall shear, as shown Figure 6, it may be observed more clearly that adverse pressure causes a vigorous response of the streamwise fluctuations across the outer and logarithmic regions of the boundary layer. This points to the presence of large-scale coherent motions, which are presumed to be responsible for the observed behavior. Additionally, normal fluctuations showed a similar, but less pronounced response to the presence of adverse pressure as shown in Figure 7. These findings serve to illustrate how viscous effects propagate in the flow direction more readily than normal to the wall. In general, fluctuations in both directions reached a maximum value at a wall-normal distance, which increased with increasing adverse-pressure-gradient for the two cases investigated. Interestingly, the data collected nearest to the wall under moderate APG conditions ($\beta=1.8$) confirmed the existence of an inflection point in both streamwise and normal profiles at approximately $y^+=70$.

Temperature Measurements

Mean Flow Field. Current results shown in Figure 8, which were found in accordance with those of Blackwell et al. (1972), suggest that the presence of adverse pressure reduced the slope of the normalized mean temperature T^+ profile in the logarithmic region. The effect of a potentially underestimated wall shear, as discussed above, by Clauser's technique for a given APG condition extends beyond the velocity field since u^* is commonly used as a normalization factor for temperature as well. Thus, the suggested slope reduction may be even more pronounced than that illustrated at this point. Present findings were described satisfactorily by a

thermal law-of-the-wall expression with constants 0.418 and 3.22 and a uniform Turbulent Prandtl Number, Pr_t , value of 0.93 across the boundary layer. However, we point to the experimental evidence available in the literature [Blackwell et al. (1972) and Ayala et al. (1997)], which has shown that Pr_t is not constant, but rather varies slightly as a function of wall-normal distance and APG condition.

Fluctuating Flow Field. Normalized fluctuations for ZPG flow are shown in Figure 9 where the present semi-log t'/T^* distribution in the thermal “core” ($80 < y^+ < 700$) was in reasonable agreement with findings by Orlando et al. (1974) and Subramanian and Antonia (1981). Discrepancies in the absolute magnitudes of the distributions may be due to differences in the development of the thermal boundary layer core region. The boundary conditions used by both references corresponded to lower free-stream flow speeds and higher wall-to-free-stream temperature differences relative to present conditions. However, more significantly, the origins of their dynamic and thermal boundary-layer fields coincided; a boundary condition not met in the present investigation. Figure 10 summarizes the tendency of adverse pressure to suppress the normalized temperature fluctuations across the logarithmic layer, which is a direct result of the decrease in wall shear with increasing adverse pressure. Consequently, the similarity of the t'/T^* profiles in the outer flow region ($y^+ > 700$) illustrates that viscous effects on the thermal field are confined approximately to the same flow region of the boundary layer near the wall as effects on the dynamic field. In addition, similar to the velocity field, the temperature fluctuations were observed to increase as the wall was approached and to dissipate quickly with increasing wall-normal distance.

Reynolds Stress Measurements

The Reynolds stress production $\overline{u'v'}$ was measured by the X-wire component of the single triple-sensor probe described previously. Findings are illustrated in normalized form in Figure 11 for the constant pressure case and for the two APG cases investigated. The existence of a constant-stress layer found under constant-pressure conditions was confirmed by the $\beta = 0$ profile. And, as adverse pressure increased, there was a corresponding increase in the stress production throughout the logarithmic region of the boundary layer. Under moderate adverse-pressure-gradient conditions, the maximum normalized turbulent stress production nearly doubled relative to the constant pressure case and occurred at approximately $y^+ = 300$. Such increase in $\overline{u'v'}$ for APG flows corresponded roughly to a similar increase observed for the u'/u^* fluctuations presented earlier. This suggests presumably that the presence of adverse pressure conditions were balanced by a proportional increase in stress generated by large-scale coherent structures in the boundary layer in order to maintain equilibrium. Turbulent stress results were confirmed, in part, by comparisons to published data such as that shown in Figure 12. And reasonable agreement is shown between present results and those of Lin (1995) and Koskie and Tiederman (1991). APG effects were confined to the core region of the boundary layer and dissipated rapidly in the outer flow as suggested by the similarity of the profiles for $y^+ > 700$.

Heat Flux Measurements

The normal and streamwise turbulent heat flux profiles illustrated in Figure 13 were approximately self-similar for the three pressure conditions investigated. Inspection of the $\beta = 0$ results for $\overline{u'v'}$ and $\overline{t'v'}$ presented in Figures 11 and 13, respectively, indicates that the Reynolds

analogy for ZPG flow was confirmed. Clearly, the similarity of the normalized distributions $\overline{u'v'}$ and $\overline{t'v'}$ under ZPG conditions support this idea, which states, roughly, that the mechanisms for shear production and heat transfer are similar. In the case of adverse pressure gradient flows, the Reynolds analogy varies as a function of pressure gradient. And, indeed, current observations suggest a Reynolds stress $\overline{u'v'}$ production mechanism, which in moderate adverse-pressure-gradient flow, scales more appropriately with the streamwise heat flux $\overline{t'u'}$ rather than with $\overline{t'v'}$. The production of heat flux was observed to occur in the core flow region for $y^+ < 700$.

Measurement Uncertainty

The standard methodology presented originally by Kline and McClintock and described in Holman, (1989) for quantifying uncertainties in single-sample experiments was applied to the mean values for the current results. These uncertainties were estimated with 20:1 odds. The statistical error uncertainties of the fluctuating quantities were estimated similarly by considering the scatter observed in the measurements. Typically, the wall-normal distance was measured within 2% accuracy. The uncertainty in the mean velocity u and v and temperature T fields also was approximately 2%, while the uncertainty associated with the fluctuating components u' , v' and t' was slightly higher in the 5% range. The turbulent flux measurements $\overline{t'u'}$, $\overline{t'v'}$, and $\overline{u'v'}$ and the normalizing scales u^* and T^* contained an uncertainty of 6%. The wall temperature measurements varied $\pm 0.5^\circ\text{C}$.

CONCLUSIONS

The characteristics of momentum and energy transport in a slightly-heated turbulent boundary layer with a step change in surface temperature were presented. Findings may be summarized as follows: *i*) the departure of the normalized mean velocity profile from the universal law-of-the-wall was not pronounced for the moderate pressure gradient cases investigated when u^* was based on Clauser's technique, *ii*) The logarithmic slope of the normalized mean temperature showed a slight decrease as adverse pressure increased, *iii*) the equilibrium condition of the flow was maintained through the balance of adverse pressure by a proportional increase in stress. This was made evident by the response of the streamwise fluctuations and the turbulent stress distributions to the presence of adverse pressure, *iv*) The Reynolds analogy was supported for ZPG conditions while, in adverse pressure, the turbulent stress production scaled with the streamwise heat flux; *v*) The heat flux was found to be self-similar for the pressure gradient cases investigated.

NOMENCLATURE

u'	fluctuating streamwise velocity
v'	fluctuating normal velocity
t'	fluctuating temperature
$\overline{t'u'}$	streamwise heat flux
T_∞	freestream temperature
ΔT	temperature difference, $= T_w - T_\infty$
$\overline{t'v'}$	normal heat flux
dP/dx	streamwise pressure gradient

u^*	friction speed, $= \sqrt{\tau_{wall}/\rho}$
T_w	wall temperature
u	streamwise instantaneous velocity
β	Clauser's equilibrium parameter, $= (\delta^*/\tau_w)dP/dx$ (also beta)
v	normal velocity
Δ	Clauser's thickness, $= \int_0^\infty \frac{U_\infty - U}{u^*} dy$
$\Delta-T$	Clauser's thermal thickness, $= \int_0^\infty \frac{T_\infty - T}{T^*} dy$
T	temperature
δ	dynamic boundary layer thickness
θ	momentum thickness
δ_T	thermal layer thickness
$\overline{u'v'}$	Reynolds shear stress
y^+	wall-normal distance
Re_θ	Momentum-deficit Reynolds number (also $Re-m$)
Re_x	Local streamwise Reynolds number
St	Stanton number, $= \frac{q_{wall}''}{\rho c_p U_\infty \Delta T}$

REFERENCES

1. Nagano, Y., Tagawa, M. and Tsuji, T., "Effects of Adverse Pressure Gradients on Mean Flow and Turbulence Statistics in a Boundary Layer," Proceedings of the 8th Symposium on Turbulent Shear Flow, Munich, September, 1991, pp. 7-21.
2. Sparlart, P.R. and Watmuff, J.H., "Experimental and Numerical Study of a Turbulent Boundary Layer with Pressure Gradients," J. Fluid Mechanics, Vol. 249, 1993, pp. 337-371.
3. Ayala, A., White, B.R. and Bagheri, N., "Turbulent Prandtl Number Measurements in Adverse Pressure Gradient Equilibrium Boundary Layers," Proceedings of the 2nd International Symposium on Turbulence, Heat and Mass Transfer, Delft, The Netherlands, June, 1997, pp. 137-146.
4. Lin, W., White, B.R. and Bagheri, N., "Experiments on the Large-scale Structure of Turbulent Boundary Layers with Adverse Pressure Gradients," AIAA Paper 95-0021, Jan. 1995.
5. Watmuff, J.H., "An Experimental Investigation of a Low Reynolds Number Turbulent Boundary Layer Subject to an Adverse Pressure Gradient," Annual Research Briefs, NASA/Stanford Center for Turbulence Research, 1989.
6. Lian, Q.X., "A Visual Study of the Coherent Structure of the Turbulent Boundary Layer in Flow with Adverse Pressure Gradient," J. of Fluid Mechanics, Vol. 215, 1990, pp. 101-124.

7. Nagano, Y., Tsuji, T., and Houra, T., "Structure of turbulent boundary layer subjected to adverse pressure gradient," Int. J. of Heat and Fluid Flow, Vol. 19, No. 5, 1998, pp. 563-572.
8. Nagano, Y. and Tagawa, M., "Statistical characteristics of wall turbulence with a passive scalar," J. Fluid Mech., Vol. 196, pp. 157-185, 1988.
9. Blackwell, B.F., Kays, W.M. and Moffat, R.J., "The Turbulent Boundary Layer on a Porous Plate: An Experimental Study of the Heat Transfer Behavior With Adverse Pressure Gradients," Report No. HMT-16, Thermosciences Division, Dept. of Mechanical Engineering, Stanford Univ., Stanford, CA, August, 1972.
10. Orlando, A.F., Moffat, R.J. and Kays, W.M., "Turbulent Transport of Heat and Momentum in a Boundary Layer Subject to Deceleration, Suction, and Variable Wall Temperature," Report No. HMT-17, Thermosciences Division, Dept. of Mechanical Engineering, Stanford Univ., Stanford, CA, 1974.
11. Bagheri, N., White, B.R., Lin, W., and Ayala, A., "Adverse-Pressure-Gradient Thermal Structure For Constant Wall Temperature Turbulent Boundary Layer," AIAA Paper 95-0022, Jan., 1995.
12. Clauser, F.H., "Turbulent Boundary Layers in Adverse Pressure Gradients," J. of Aero. Sci., Vol. 21, 1954, pp.91-105.
13. Subramanian, C.S. and Antonia, R.A., "Effect of Reynolds Number on a Slightly Heated Turbulent Boundary Layer," Int. J. of Heat and Mass Transfer, Vol. 24, No. 11, 1981, pp. 1833-1846.
14. Lin, W., Experiments on the Large-Scale Structure of Turbulent Boundary Layers with Adverse-Pressure-Gradient, Ph.D. thesis, Department of Mechanical and Aeronautical Engineering, University of California, Davis, 1995.
15. Koskie, J.E. and Tiederman, W.G., "Turbulent Structure and Polymer Drag Reduction I Adverse Pressure Gradient Boundary Layers," PME-FM-91-3, Office of Naval Research, 1991.
16. Holman, J.P., Experimental Methods for Engineers, 5th Ed., McGraw-Hill, New York, 1989.

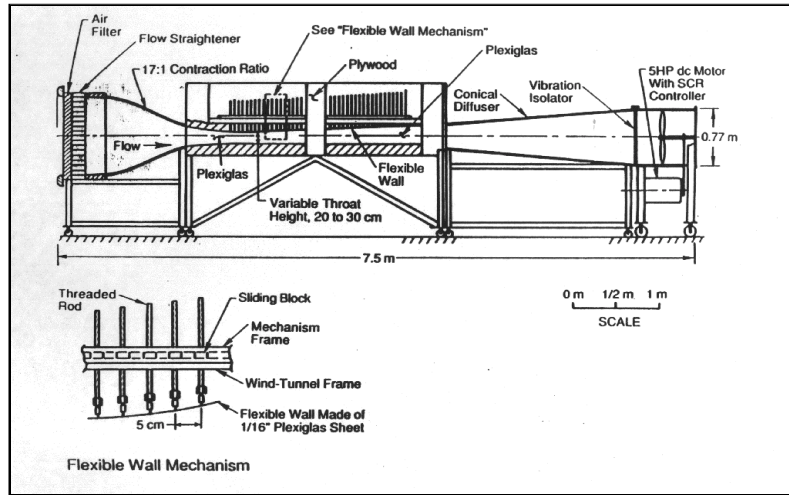


Figure 1. Schematic of the APG wind-tunnel facility at UC Davis.

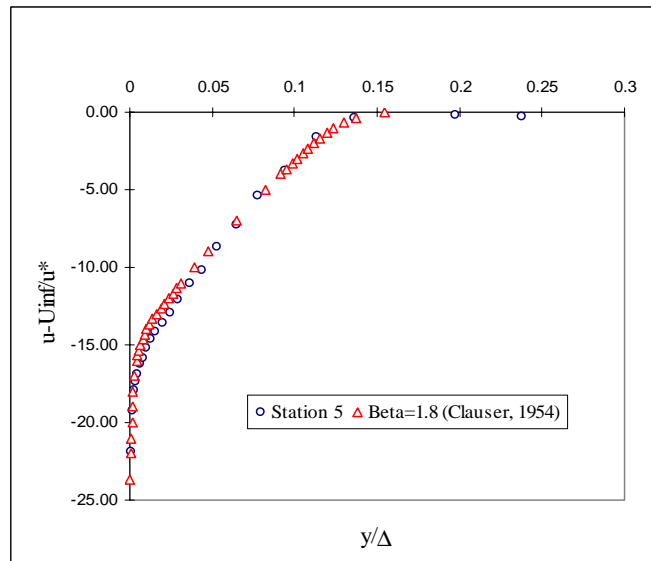


Figure 2. Velocity-defect check for moderate APG ($\beta=1.8$), $\Delta T=0$ flow conditions

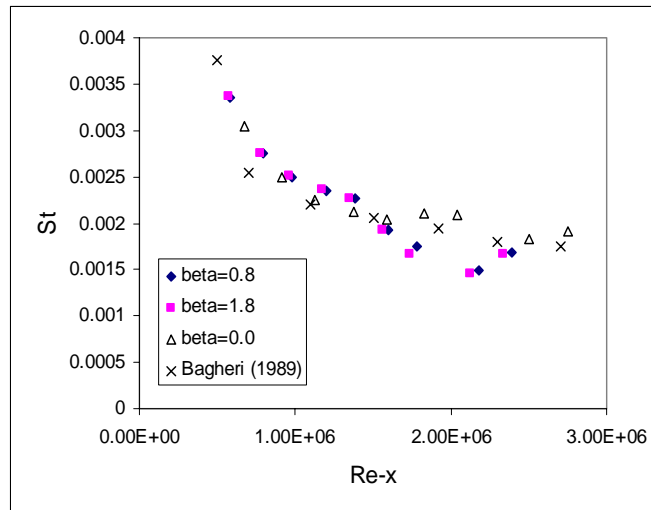


Figure 3. Stanton number distribution along wind tunnel wall.

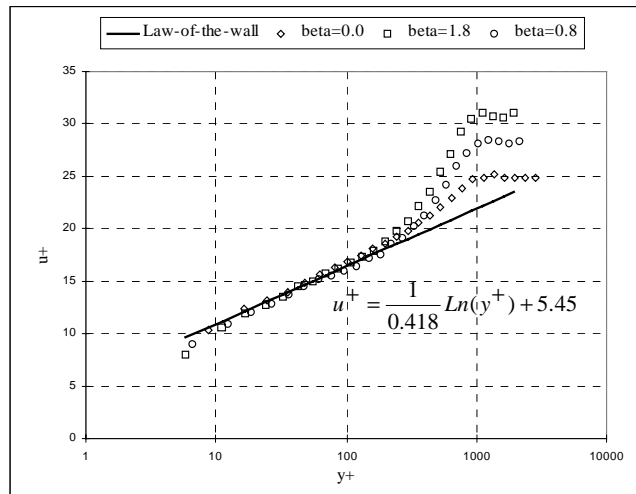


Figure 4. Mean velocity profile in ZPG and APG conditions.

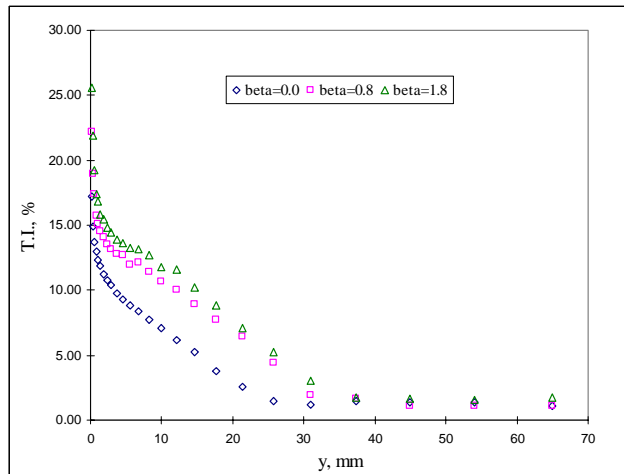


Figure 5. Turbulence intensity distributions for ZPG, mild, and moderate APG.

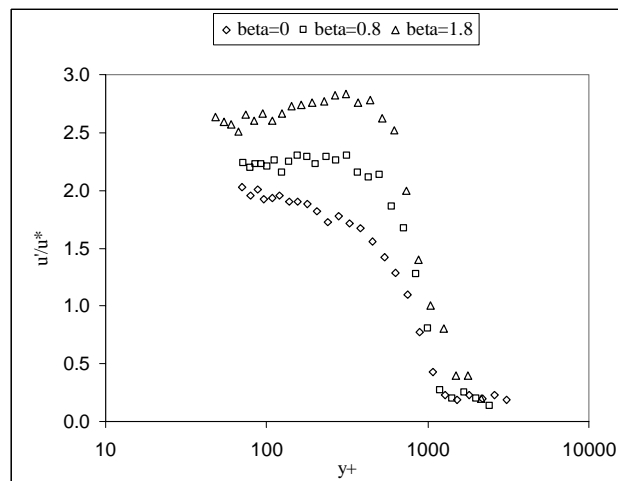


Figure 6. Streamwise velocity fluctuations for ZPG and APG.

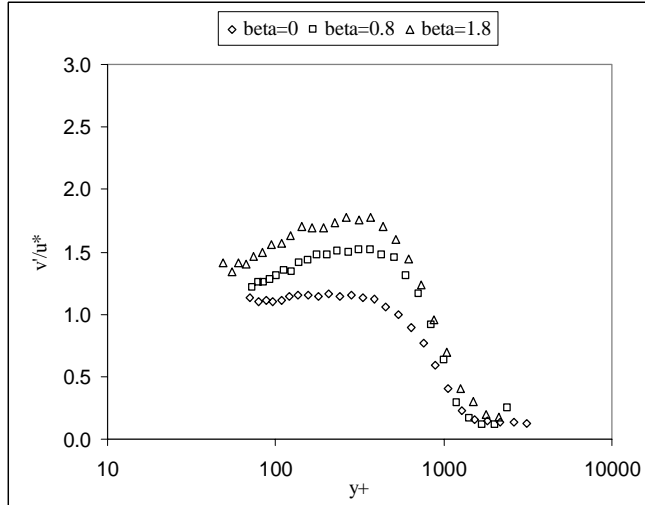


Figure 7. Normal velocity fluctuations for ZPG and APG.

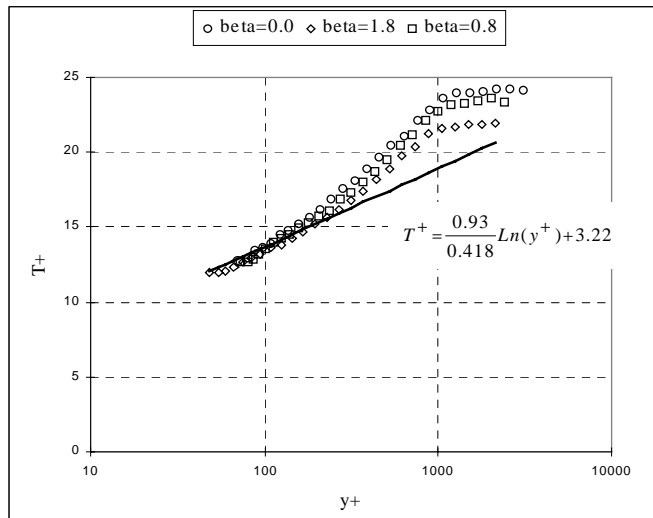


Figure 8. Mean temperature profile in ZPG and APG conditions.

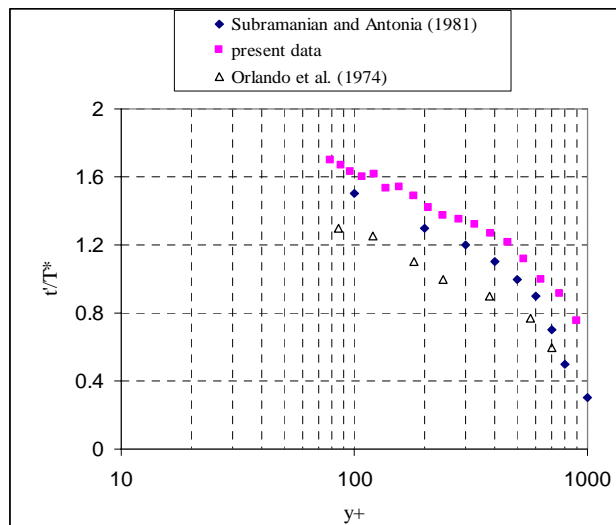


Figure 9. Comparison of temperature fluctuations in ZPG conditions.

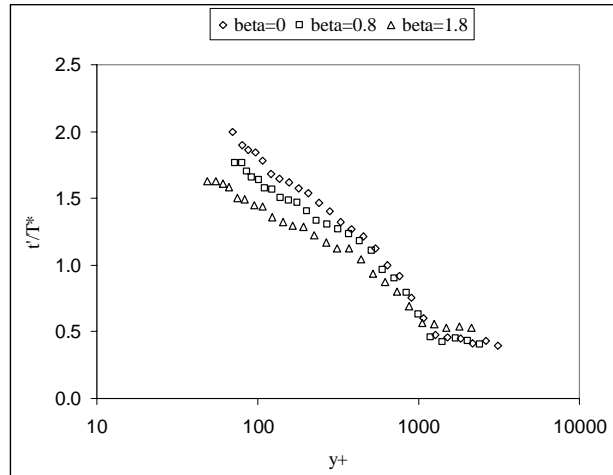


Figure 10. Temperature fluctuations profile in ZPG and APG conditions.

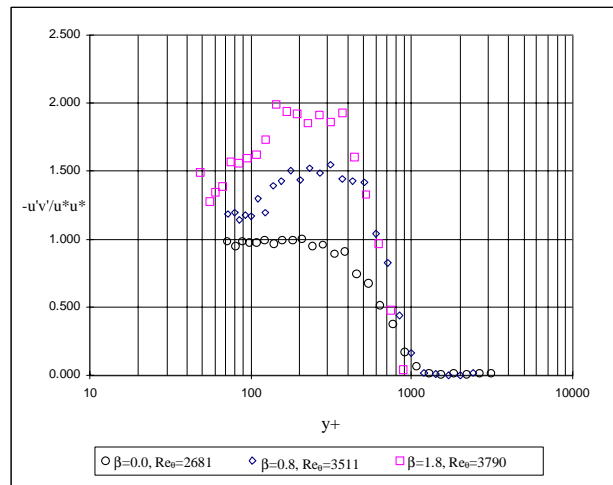


Figure 11. Turbulent stress production in ZPG and APG conditions.

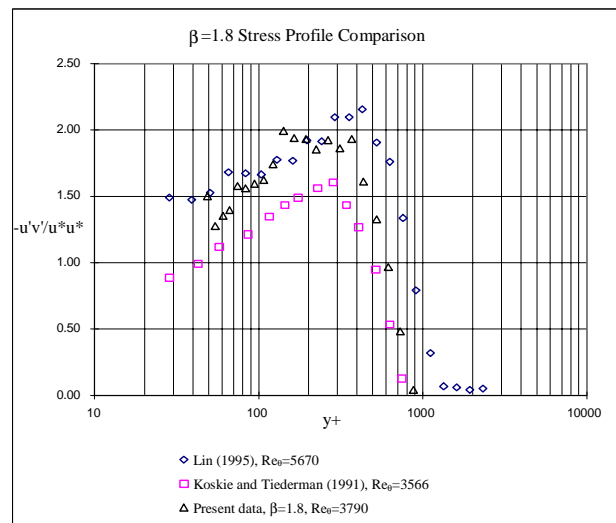


Figure 12. Comparison of turbulent stress production in moderate APG conditions.

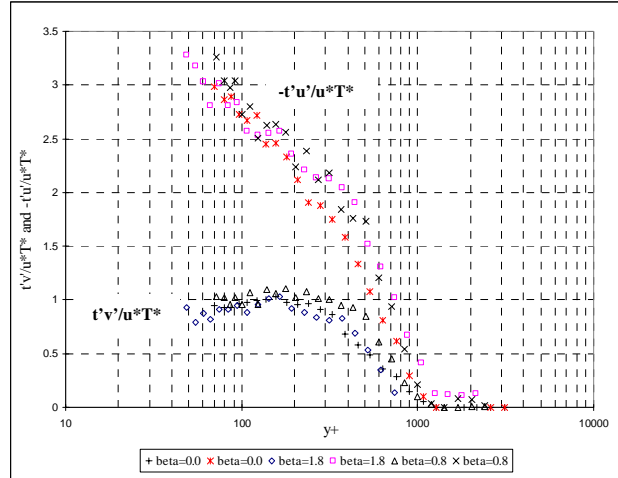


Figure 13. Turbulent heat flux distributions in ZPG and APG conditions.

β	u^*	U_∞	Re_θ	T^*	δ	δ^*	θ	ΔT	Δ	$\Delta-T$
	m/s	m/s			mm	mm	mm	°C	mm	mm
0.0	0.70	17.5	2681	0.67	20	3.0	2.3	11.5	75.1	93.0
0.8	0.54	15.3	3511	0.70	25	4.7	3.4	11.8	134.1	108.7
1.8	0.48	14.9	3790	0.75	30	5.4	3.8	11.8	165.4	110.2

Table 1. Test Parameters.